LSQR-BASED ICI EQUALIZATION FOR MULTICARRIER COMMUNICATIONS IN STRONGLY DISPERSIVE AND HIGHLY MOBILE ENVIRONMENTS

Georg Tauböck[a], *Mario Hampejs*[b], *Gerald Matz*[a], *Franz Hlawatsch*[a], *and Karlheinz Gröchenig*[b]

[a]Institute of Communications and Radio-Frequency Engineering, Vienna University of Technology
Gusshausstrasse 25/389, A-1040 Vienna, Austria; e-mail: gtauboec@nt.tuwien.ac.at

[b]Numerical Harmonic Analysis Group, Faculty of Mathematics, University of Vienna
Nordbergstrasse 15, A-1090 Vienna; e-mail: karlheinz.groechenig@univie.ac.at

ABSTRACT

For OFDM transmission over rapidly varying channels, intercarrier interference (ICI) constitutes a major source of performance degradation. We propose a low-complexity ICI equalization technique that uses the iterative LSQR algorithm for regularized inversion of a triple-band approximation to the frequency-domain channel matrix. The LSQR algorithm achieves regularization of the (typically ill-conditioned) channel inversion via early termination of the iteration process, and thus yields good results at low complexity. We also consider pulse shaping as a means of reducing the bandwidth of the matrix approximation. Simulation results demonstrate the excellent performance of the proposed ICI equalizer even for strongly dispersive and rapidly varying channels, as well as the potential of pulse shaping for reducing the "ICI bandwidth."

1. INTRODUCTION

Orthogonal frequency division multiplexing (OFDM) is an attractive multicarrier (MC) modulation scheme for broadband wireless communications [1]. Recently, there has been increasing interest in scenarios where the channel changes noticeably within an OFDM symbol due to user mobility and/or carrier frequency offsets. An example is mobile reception of DVB-T (e.g. [2]), which was originally conceived for fixed receivers. In highly mobile scenarios, large Doppler shifts cause strong intercarrier interference (ICI), which constitutes a major source of performance degradation.

Several techniques for combating ICI have been proposed. *Pulse-shaping OFDM* or *biorthogonal frequency division multiplexing* (BFDM) [3] generalize classical cyclic-prefix OFDM by allowing the use of nonrectangular transmit and receive pulses. Smooth pulses can cause a substantial reduction of ICI [3, 4]. Other approaches concern only the receiver processing to remain compliant with existing OFDM standards. They are motivated by the observation that, for strong ICI, conventional *single-tap* equalization in the frequency (subcarrier) domain suffers from an error floor because the performance becomes ICI-limited above a certain SNR threshold (see [4–8] for an analysis of ICI effects on receiver performance).

For ICI reduction, therefore, frequency-domain equalizers processing all subcarriers [9] or a few neighboring subcarriers [8] simultaneously have been proposed. The latter approach saves computations and amounts to approximating the frequency-domain channel matrix by a banded matrix. The banded matrix approach has been combined with an LDL factorization in [10]. Further methods involve an "ICI-shaping" concentrating the ICI power within a small matrix band [11], or use a linear approximation of the channel variations [2, 12].

This work was supported by WWTF project MA 44 (MOHAWI).

In contrast to these frequency-domain methods, a recently proposed linear equalization and ICI mitigation technique [13] operates in the time domain. By processing the received signal before FFT demodulation, it is able to exploit the *strict* band structure of the time-domain channel matrix. The technique uses the iterative *LSQR algorithm* [14], which has excellent performance at low complexity due to its ability to regularize the (typically ill-conditioned) channel inversion problem by early termination of the iterations. More specifically, the complexity order per iteration is $\mathcal{O}(KM)$ operations, where K is the number of subcarriers and M is the maximum delay of the channel. Thus, the method is particularly attractive when the channel's maximum delay is not too large.

In this paper, we address the case of (potentially) large channel delays, for which the time-domain LSQR equalizer has a higher complexity. For large channel delays, it is more efficient to use a banded matrix model in the frequency domain than in the time domain. Therefore, we propose an equalizer that combines the advantages of the LSQR algorithm with the efficiency of a frequency-domain band approximation. The complexity of this equalizer is lower when the ICI is effectively constrained to a small band. Therefore, we also consider *pulse-shaping* MC modulation (with smooth pulses) as a means to reduce the "ICI bandwidth."

The main contributions and the organization of this paper are as follows. The system model is presented in Section 2. An analysis of intersymbol interference (ISI) and ICI for pulse-shaping MC transmission is performed in Section 3. This analysis shows the potential of smooth pulses to reduce the effective ICI bandwidth and, thus, the complexity of frequency-domain ICI equalizers using a band approximation. In Section 4, the frequency-domain LSQR equalizer is presented and the main steps of the LSQR algorithm are described. Finally, simulation results provided in Section 5 compare the performance of the proposed equalizer with that of its time-domain counterpart and demonstrate the benefit of pulse shaping.

2. SYSTEM MODEL

We consider a pulse-shaping MC system [3] with K subcarriers and symbol period N. As mentioned above, pulse shaping allows the use of smooth transmit and receive pulses, which can reduce ICI. We emphasize that conventional cyclic-prefix OFDM is a simple special case of our setting, corresponding to rectangular pulses.

2.1. Equivalent system channel

The MC modulator produces the (equivalent baseband) transmit signal

$$s(n) = \sum_{l=-\infty}^{\infty} \sum_{k=0}^{K-1} a_{l,k}\, g_{l,k}(n)\,, \tag{1}$$

where $a_{l,k}$ with $l \in \mathbb{Z}$, $k \in \{0, \ldots, K-1\}$ denotes the data symbols,

$$g_{l,k}(n) \triangleq g(n-lN)\, e^{j2\pi \frac{k}{K}(n-lN)}$$

is a time-frequency shifted version of a transmit pulse $g(n)$, and $n \in \mathbb{Z}$. Assuming a time-varying and time-dispersive (frequency-selective) channel, the received signal is

$$r(n) = (\mathbb{H}s)(n) + z(n) = \sum_{m=0}^{M} h(n,m)\, s(n-m) + z(n)\,, \tag{2}$$

where $h(n,m)$ denotes the time-varying impulse response of the channel $\mathbb{H}$, M is the maximum channel delay, and $z(n)$ is noise. Finally, the MC demodulator computes the inner products

$$x_{l,k} = \langle r, \gamma_{l,k} \rangle = \sum_{n=-\infty}^{\infty} r(n)\, \gamma_{l,k}^*(n)\,, \tag{3}$$

where $\gamma_{l,k}(n) \triangleq \gamma(n-lN)\, e^{j2\pi \frac{k}{K}(n-lN)}$ is a time-frequency shifted version of a receive pulse $\gamma(n)$. For rectangular pulses

$$g(n) = \begin{cases} 1, & -(N-K) \le n \le K-1 \\ 0, & \text{otherwise} \end{cases} \tag{4}$$

$$\gamma(n) = \begin{cases} 1, & 0 \le n \le K-1 \\ 0, & \text{otherwise}\,, \end{cases} \tag{5}$$

the pulse-shaping MC system reduces to conventional OFDM with cyclic prefix length $N-K \ge 0$.

Combining (1), (2), and (3), we obtain the following relation between the transmit symbols $a_{l,k}$ and receive symbols $x_{l,k}$ [3]:

$$x_{l,k} = \sum_{l'=-\infty}^{\infty} \sum_{k'=0}^{K-1} H_{l,k;l',k'}\, a_{l',k'} + z_{l,k}\,, \tag{6}$$

with

$$H_{l,k;l',k'} = \langle \mathbb{H}\, g_{l',k'}, \gamma_{l,k} \rangle \tag{7}$$

$$= \sum_{n=-\infty}^{\infty} \sum_{m=0}^{M} h(n+lN, m)\, g(n-m+(l-l')N)\, \gamma^*(n) \cdot e^{j\frac{2\pi}{K}[k'(n-m+(l-l')N) - kn]} \tag{8}$$

and

$$z_{l,k} = \langle z, \gamma_{l,k} \rangle\,.$$

The coefficients $H_{l,k;l',k'}$ describe the "system channel" that subsumes the MC modulator, the doubly spread physical channel, and the MC demodulator. In general, this system channel introduces both ISI (characterized by $H_{l,k;l',k'}$ for $l \ne l'$) and ICI (characterized by $H_{l,k;l',k'}$ for $k \ne k'$).

2.2. Frequency-domain channel matrix

Consider a transmit pulse $g(n)$ and receive pulse $\gamma(n)$ such that the support of $g(n)$ extended by the maximum channel delay M does not overlap with the support of $\gamma(n)$ shifted by nonzero multiples of the symbol period N. This condition is satisfied, in particular, in the case of cyclic-prefix OFDM (see (4), (5)) provided that $M \le N-K$. For such pulses, it follows from (8) that the ISI is zero, i.e.,

$$H_{l,k;l',k'} = 0 \quad \text{for } l \ne l'.$$

As a consequence, the system channel can be completely described by the sequence of *frequency-domain channel matrices* $\mathbf{H}^{(l)}$ of size $K \times K$ defined as $(\mathbf{H}^{(l)})_{k,k'} \triangleq H_{l,k;l,k'}$ with $k,k' = 0,\ldots,K-1$. The system channel input-output relation (6) can then be compactly written as

$$\mathbf{x}^{(l)} = \mathbf{H}^{(l)}\mathbf{a}^{(l)} + \mathbf{z}^{(l)}, \qquad l \in \mathbb{Z}\,, \tag{9}$$

with the vectors $\mathbf{x}^{(l)} \triangleq [x_{l,0} \cdots x_{l,K-1}]^T$, $\mathbf{a}^{(l)} \triangleq [a_{l,0} \cdots a_{l,K-1}]^T$, and $\mathbf{z}^{(l)} \triangleq [z_{l,0} \cdots z_{l,K-1}]^T$. The ICI is described by the *off-diagonal* entries of the channel matrices $\mathbf{H}^{(l)}$, which can be expected to become small if they are sufficiently distant from the main diagonal. This suggests to approximate $\mathbf{H}^{(l)}$ by a *banded matrix* [8, 10].

Later, we shall consider smooth pulses $g(n)$ and $\gamma(n)$ that do not satisfy the above support condition exactly but are fast decaying outside a suitable time interval. For such pulses, there will be some ISI, which is not described by the frequency-domain model (9). Therefore, (9) will be merely an approximation. The ISI will lead to a performance degradation if equalization is based on (9), that is, if only the ICI is equalized, without an attempt to equalize also the ISI. On the other hand, the smoothness of the pulses can be expected to lead to a smaller "effective ICI bandwidth" of $\mathbf{H}^{(l)}$, which may result in a reduction of equalizer complexity. We will next investigate this issue in a stochastic setting.

3. ISI/ICI ANALYSIS

In this section, we analyze the *mean ISI/ICI power* for a random channel and demonstrate the potential of smooth transmit and receive pulses for ICI reduction.

3.1. Delay-Doppler formulation of the system channel

We first develop a different representation of the system channel coefficients $H_{l,k;l',k'}$. The effect of the channel $\mathbb{H}$ in (2) can be expressed in terms of the delay (m) and Doppler (ξ) variables as

$$(\mathbb{H}s)(n) = \sum_{m=0}^{M} \int_{-1/2}^{1/2} S_{\mathbb{H}}(m,\xi)\, s(n-m)\, e^{j2\pi\xi n}\, d\xi\,, \tag{10}$$

with the *spreading function* [15]

$$S_{\mathbb{H}}(m,\xi) \triangleq \sum_{n=-\infty}^{\infty} h(n,m)\, e^{-j2\pi\xi n}.$$

Using the *cross-ambiguity function* [16]

$$A_{\gamma,g}(m,\xi) \triangleq \sum_{n=-\infty}^{\infty} \gamma(n)\, g^*(n-m)\, e^{-j2\pi\xi n},$$

the system channel coefficients in (7) can then be expressed as

$$H_{l,k;l',k'} = \sum_{m=0}^{M} \int_{-1/2}^{1/2} S_{\mathbb{H}}(m,\xi)\, A^*_{\gamma_{l,k},\, g_{l',k'}}(m,\xi)\, d\xi$$
$$= e^{-j2\pi\frac{N}{K}k'(l'-l)} \sum_{m=0}^{M} \int_{-1/2}^{1/2} e^{-j2\pi(m\frac{k'}{K} - \xi lN)} \cdot S_{\mathbb{H}}(m,\xi)\, A^*_{\gamma,g}\Big(m+(l'-l)N, \xi+\frac{k'-k}{K}\Big)\, d\xi\,, \tag{11}$$

where we have used (10) and the relation $A_{\gamma_{l,k},\, g_{l',k'}}(m,\xi) = e^{j2\pi[\frac{N}{K}k'(l'-l) + m\frac{k'}{K} - \xi lN]}\, A_{\gamma,g}\big(m+(l'-l)N,\, \xi+\frac{k'-k}{K}\big)$.

3.2. Mean ISI/ICI power

We now adopt a simple stochastic structure for the channel $\mathbb{H}$. We assume that the impulse response samples $h(n,m)$ are zero-mean, rotationally invariant (or proper or circularly symmetric), jointly complex Gaussian variables. We furthermore assume that the second-order statistics of the channel conform to the *wide-sense stationary uncorrelated scattering* (WSSUS) property [15]

$$\mathrm{E}\big\{S_{\mathbb{H}}(m,\xi)\, S^*_{\mathbb{H}}(m',\xi')\big\} = C_{\mathbb{H}}(m,\xi)\, \delta^{(1)}(\xi-\xi')\, \delta[m-m']\,, \tag{12}$$

where $C_{\mathbb{H}}(m,\xi)$ is the channel's scattering function [15], $\delta^{(1)}(\cdot)$ is the Dirac impulse periodized with period 1, and $\delta[\cdot]$ is the unit sample. Finally, we assume a maximum delay M and a maximum Doppler shift $\pm\xi_{\max}/2$, i.e., the support of $C_{\mathbb{H}}(m,\xi)$ (within the fundamental ξ-interval $[-1/2, 1/2)$) is contained in the rectangle $\{0,\dots,M\}\times[-\xi_{\max}/2, \xi_{\max}/2]$.

The *mean ISI/ICI power* is defined as $\mathrm{E}\{|H_{l,k;l',k'}|^2\}$ for $l\neq l'$ or $k\neq k'$ (or both). Using (11) and (12), we obtain

$$\mathrm{E}\{|H_{l,k;l',k'}|^2\} = \sum_{m=0}^{M}\int_{-\xi_{\max}/2}^{\xi_{\max}/2} C_{\mathbb{H}}(m,\xi) \cdot \left|A_{\gamma,g}\Big(m+(l'-l)N, \xi+\frac{k'-k}{K}\Big)\right|^2 d\xi. \quad (13)$$

We also consider the *mean ICI power* defined as the mean power of the entries on the qth off-diagonal of the frequency-domain channel matrix $\mathbf{H}^{(l)}$,

$$P(q) \triangleq \mathrm{E}\{|(\mathbf{H}^{(l)})_{k,k+q}|^2\} = \mathrm{E}\{|H_{l,k;l,k+q}|^2\} = \sum_{m=0}^{M}\int_{-\xi_{\max}/2}^{\xi_{\max}/2} C_{\mathbb{H}}(m,\xi)\,\Big|A_{\gamma,g}\Big(m,\xi+\frac{q}{K}\Big)\Big|^2 d\xi. \quad (14)$$

This does not depend on l or k. We note the periodicity property $P(q+K)=P(q)$, from which one can conclude that if $P(q)$ decreases for growing $|q|$ on the interval $0\le|q|\le K/2$, it will increase for $K/2\le|q|\le K-1$.

For classical cyclic-prefix OFDM, that is, for the rectangular pulses in (4) and (5), one obtains

$$|A_{\gamma,g}(m,\xi)|^2 = \begin{cases} \frac{\sin^2(\pi(m+K)\xi)}{\sin^2(\pi\xi)}, & -K+1\le m\le -1 \\ \frac{\sin^2(\pi K\xi)}{\sin^2(\pi\xi)}, & 0\le m\le N-K \\ \frac{\sin^2(\pi(N-m)\xi)}{\sin^2(\pi\xi)}, & N-K+1\le m\le N-1 \\ 0, & \text{otherwise}. \end{cases} \quad (15)$$

Inserting (15) into (13), it is easily seen that $\mathrm{E}\{|H_{l,k;l',k'}|^2\}=0$ for $l\neq l'$ provided that $M\le N-K$, which again indicates the total absence of ISI. Inserting (15) into (14) while still assuming $M\le N-K$ yields for the ICI power

$$P(q) = \sum_{m=0}^{M}\int_{-\xi_{\max}/2}^{\xi_{\max}/2} C_{\mathbb{H}}(m,\xi)\,\frac{\sin^2(\pi K\xi)}{\sin^2\big(\pi(\xi+\frac{q}{K})\big)}\,d\xi, \quad (16)$$

where $\sin^2\big(\pi K(\xi+\frac{q}{K})\big)=\sin^2(\pi K\xi)$ has been used. It is easy to see that there are channels where $P(q)$ has a comparatively poor decay. For example, for a single-scatterer channel with scattering function $C_{\mathbb{H}}(m,\xi)=c\,\delta[m-m_0]\,\delta^{(1)}(\xi-\xi_0)$, (16) yields

$$P(q) = c\,\frac{\sin^2\big(\pi K\xi_0\big)}{\sin^2\big(\pi(\xi_0+\frac{q}{K})\big)} \ge c\,\frac{\sin^2\big(\pi K\xi_0\big)}{\big[\pi(\xi_0+\frac{q}{K})\big]^2}.$$

This shows that the ICI decay with respect to q, within $0\le|q|\le K/2$, is not quite of second order.

Much better ICI decay can be obtained with pulse-shaping MC systems using suitable smooth pulses. Indeed, it is shown in [4] that there exist perfect-reconstruction pulses (i.e., pulses such that $x_{l,k}=a_{l,k}$ for a distortionless and noiseless channel) yielding a polynomially or even (sub-)exponentially decaying cross-ambiguity function $A_{\gamma,g}(m,\xi)$ and, hence, an ISI/ICI decay of the same characteristic. As an example, Fig. 1 compares $P(q)$ (normalized by $P(0)$) for the rectangular pulses (4), (5) and for smooth pulses whose construction is described in Section 5.2 along with the system and channel parameters in force. It is seen that the off-diagonal decay of the frequency-domain channel matrix within $0\le|q|\le K/2$ is much faster for the smooth pulses than for the rectangular pulses.

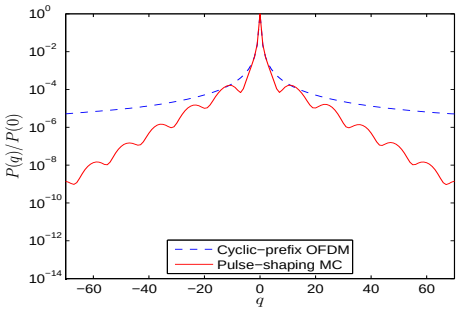

Fig. 1. *Normalized mean ICI power $P(q)$ versus the off-diagonal index q for the rectangular pulses (4), (5) and for smooth pulses.*

4. FREQUENCY-DOMAIN LSQR EQUALIZER

We now describe the proposed technique for ICI mitigation through equalization of a banded approximation to the frequency-domain channel matrix $\mathbf{H}^{(l)}$. Hereafter, we consider $\mathbf{H}^{(l)}$ for a fixed symbol time l and hence suppress the superscript $^{(l)}$.

4.1. The proposed equalizer

Because $\mathbf{H}$ may have a very high condition number—particularly for channels with large maximum delay and Doppler—, zero-forcing (ZF) equalization performs poorly and some kind of regularization (cf. [17]) has to be employed[1]. Here, we will consider the use of the LSQR algorithm [13, 14], which is an iterative algorithm for equalization with "implicit regularization."

Direct application of LSQR-based equalization to the $K\times K$ frequency-domain channel matrix $\mathbf{H}$ would be quite complex. However, we know from the previous section that $\mathbf{H}$ exhibits off-diagonal decay within $0\le|q|\le K/2$ and off-diagonal growth within $K/2\le|q|\le K-1$. We can thus approximate $\mathbf{H}$ by a triple-banded matrix $\mathbf{H}_{\mathrm{B}}$ with a band of (one-sided) width B about the main diagonal and two bands of width B in the lower-left and upper-right corners:

$$(\mathbf{H}_{\mathrm{B}})_{k,k'} \triangleq \begin{cases} (\mathbf{H})_{k,k'}, & |k'-k|\le B \text{ or } K-B\le|k'-k|\le K-1 \\ 0, & \text{otherwise} \end{cases}$$

(note that $q=k'-k$). Application of the LSQR algorithm to the *sparse* matrix $\mathbf{H}_{\mathrm{B}}$ yields a significant reduction of complexity.

The LSQR algorithm is an iterative algorithm for solving least-squares problems that is specifically tailored to sparse matrices [14]. In exact arithmetic, it is equivalent to the *conjugate gradient method for the normal equations* (CGNE). However, it has advantages regarding complexity and numerical stability in fixed-point arithmetic. In our context, the normal equations are given by

$$\mathbf{H}_{\mathrm{B}}^H\mathbf{H}_{\mathrm{B}}\,\mathbf{a} = \mathbf{H}_{\mathrm{B}}^H\mathbf{x},$$

where $\mathbf{a}$ and $\mathbf{x}$ are the data symbol vector and demodulated symbol vector, respectively and $(\cdot)^H$ denotes Hermitian transposition. These normal equations are obtained from (9) by disregarding the noise $\mathbf{z}$, replacing $\mathbf{H}$ with $\mathbf{H}_{\mathrm{B}}$, and left-multiplying by $\mathbf{H}_{\mathrm{B}}^H$.

[1] Minimum mean-square error (MMSE) equalization, too, can be viewed as a regularization of ZF equalization (one that presupposes knowledge of the noise variance).

At the ith LSQR iteration, an approximate solution to the normal equations is obtained by minimizing $\|\mathbf{H}_\mathrm{B}\,\mathbf{a}-\mathbf{x}\|$ with respect to $\mathbf{a}$ subject to the constraint that $\mathbf{a}$ lies in the Krylov subspace[2] $\mathcal{K}\big(\mathbf{H}_\mathrm{B}^H\mathbf{H}_\mathrm{B}, \mathbf{H}_\mathrm{B}^H\mathbf{x}, i\big)$. Although these Krylov subspaces are generated by $\mathbf{H}_\mathrm{B}^H\mathbf{H}_\mathrm{B}$, the performance of the LSQR algorithm is governed by the condition number of $\mathbf{H}_\mathrm{B}$ and not by that of $\mathbf{H}_\mathrm{B}^H\mathbf{H}_\mathrm{B}$ (which is the square of the condition number of $\mathbf{H}_\mathrm{B}$). This is important since already the condition number of $\mathbf{H}_\mathrm{B}$ is high for channels with large delay and Doppler (the same, by the way, is true for the nonbanded channel matrix $\mathbf{H}$ and its time-domain counterpart).

The high condition number of $\mathbf{H}_\mathrm{B}$ is also the reason why a regularization is necessary. With the LSQR algorithm, the regularization is achieved by early termination of the iteration process [17]. This is because the initial iterations reduce the approximation error $\mathbf{H}_\mathrm{B}\,\mathbf{a}-\mathbf{x}$ in the directions of the dominant right singular vectors of $\mathbf{H}_\mathrm{B}$, which are less affected by noise than the directions corresponding to small singular values. There is an optimum number of LSQR iterations such that the error norm $\|\mathbf{H}_\mathrm{B}\,\mathbf{a}-\mathbf{x}\|$ is minimized, that is, most of the ICI is equalized with low noise enhancement. Fewer iterations result in larger residual ICI whereas more iterations produce stronger noise enhancement. Fortunately, the minimum usually is not very pronounced, so that moderate deviations from the optimum number of iterations do not degrade the performance significantly.

The complexity order of the LSQR algorithm is $\mathcal{O}(K(2B+1)I)$ operations, where I denotes the number of iterations used. Thus, the complexity is just linear in the number of subcarriers K, the matrix bandwidth B, and the number of iterations I. In summary, the LSQR algorithm is attractive because of its numerical stability, its inherent regularization, and its low computational complexity.

4.2. Statement of the LSQR algorithm

The two main parts of the LSQR algorithm are a Golub-Kahan bidiagonalization and a cheap QR decomposition solving a bidiagonal least squares problem. The Golub-Kahan bidiagonalization [18] is an iterative procedure that constructs vectors $\mathbf{u}_i, \mathbf{v}_i$ and positive constants α_i, β_i as follows.

1. Initialization:

$$\alpha_1 = \|\mathbf{H}_\mathrm{B}^H\mathbf{x}\|, \quad \beta_1 = \|\mathbf{x}\|, \quad \mathbf{u}_1 = \frac{\mathbf{x}}{\beta_1}, \quad \mathbf{v}_1 = \frac{\mathbf{H}_\mathrm{B}^H\mathbf{x}}{\alpha_1}.$$

2. Recursion: for $i = 1, 2, \ldots,$

$$\begin{aligned}
\alpha_{i+1} &= \|\mathbf{H}_\mathrm{B}^H\mathbf{u}_i - \beta_i\mathbf{v}_i\| \\
\beta_{i+1} &= \|\mathbf{H}_\mathrm{B}\mathbf{v}_i - \alpha_i\mathbf{u}_i\| \\
\mathbf{u}_{i+1} &= \frac{1}{\beta_{i+1}}\left(\mathbf{H}_\mathrm{B}\mathbf{v}_i - \alpha_i\mathbf{u}_i\right) \\
\mathbf{v}_{i+1} &= \frac{1}{\alpha_{i+1}}\left(\mathbf{H}_\mathrm{B}^H\mathbf{u}_i - \beta_i\mathbf{v}_i\right).
\end{aligned}$$

Theoretically, this recursion is terminated when $\alpha_{i+1} = 0$ or $\beta_{i+1} = 0$. The vectors $\mathbf{u}_i$, $i = 1, 2, \ldots$ are orthonormal, and so are the vectors $\mathbf{v}_i$, $i = 1, 2, \ldots$ They allow one to reduce the minimization problem $\min_\mathbf{a}\|\mathbf{H}_\mathrm{B}\,\mathbf{a}-\mathbf{x}\|$ over the ith Krylov subspace to the bidiagonal least-squares problem

$$\min_\mathbf{w}\|\mathbf{B}_i\mathbf{w} - \beta_1\mathbf{e}_1\|, \tag{17}$$

where $\mathbf{e}_1 = [1\ 0\ \cdots\ 0]^T$ and $\mathbf{B}_i$ is the $(i+1)\times i$ lower bidiagonal matrix with $\alpha_1, \ldots, \alpha_i$ on the main diagonal and $\beta_2, \ldots, \beta_{i+1}$ on the first subdiagonal. The ith approximate solution of the original problem is then given by

$$\mathbf{a}_i = [\mathbf{v}_1 \cdots \mathbf{v}_i]\,\mathbf{w}_i,$$

where $\mathbf{w}_i$ is the solution of (17).

The second part of the LSQR algorithm is the solution of the bidiagonal least squares problem (17) through QR factorization [18] of $\mathbf{B}_i$. The computational cost of this step is negligible because $\mathbf{B}_i$ is bidiagonal. Furthermore, [14] presents a recursion to compute $\mathbf{w}_i$ via a simple update of $\mathbf{w}_{i-1}$.

[2] The Krylov subspace $\mathcal{K}(\mathbf{A}, \mathbf{b}, i)$ is defined as the space spanned by the $i+1$ vectors $\mathbf{b}, \mathbf{A}\mathbf{b}, \ldots, \mathbf{A}^i\mathbf{b}$ [18, Section 9.1.1].

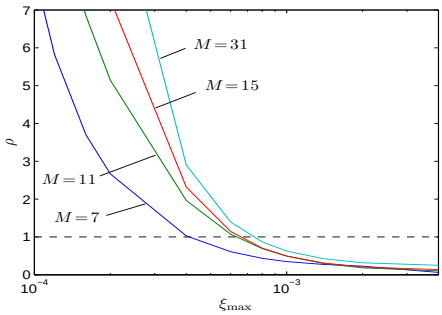

Fig. 2. *Complexity ratio $\rho = \frac{M+1}{2B+1}$ for cyclic-prefix OFDM, at almost equal coded BER of FD-LSQR and TD-LSQR equalization.*

5. SIMULATION RESULTS

We will now provide simulation results to compare the performance of the proposed equalizer with that of its time-domain counterpart and to demonstrate the benefit of pulse shaping.

5.1. Complexity comparison of frequency-domain and time-domain LSQR equalization

We first compare the complexity of the proposed frequency-domain (FD) LSQR equalizer with that of the time-domain (TD) LSQR equalizer of [13]. We simulated a cyclic-prefix OFDM system (i.e., using rectangular pulses (4), (5)) with $K = 256$ subcarriers and cyclic prefix length $N-K = 32$, whence $N = 288$. Furthermore, we used a 4-QAM symbol alphabet with Gray labeling, a rate-$1/2$ convolutional code (generator polynomial $(13_8, 15_8)$), and 32×16 row-column interleaving. A noisy WSSUS channel characterized by uniform delay and Doppler profiles (brick-shaped scattering function) with maximum delay $M = 7\ldots 31$ and maximum Doppler $\xi_\mathrm{max} = 1\cdot 10^{-4}\ldots 4\cdot 10^{-3}$ was simulated according to [19]. The given range of ξ_max corresponds to a maximum *normalized* Doppler frequency (physical Doppler frequency divided by subcarrier spacing) between 1.28% and 51.2%. We used $I = 15$ iterations for both the FD-LSQR and TD-LSQR equalizers.

The complexity of the TD-LSQR equalizer is $\mathcal{O}(K(M+1)I)$ operations, whereas that of the proposed FD-LSQR equalizer is effectively $\mathcal{O}(K(2B+1)I)$ operations. Let us define the "complexity ratio" $\rho \triangleq \frac{M+1}{2B+1}$. Roughly speaking, the FD-LSQR equalizer is less complex than the TD-LSQR equalizer for $\rho > 1$, and the other way around for $\rho < 1$. It is important to note that the matrix bandwidth B is a design parameter of the FD-LSQR equalizer that determines both its complexity and its equalization performance (better performance is typically obtained for a larger B, at the cost of a higher complexity). In particular, for $B < K/2$, the performance of TD-LSQR can be expected to be better than that of FD-LSQR because FD-LSQR uses a banded approximation to the channel matrix $\mathbf{H}$ whereas TD-LSQR always uses the full (time-domain) channel matrix. In Fig. 2, we show the complexity ratio ρ for B chosen as the minimum

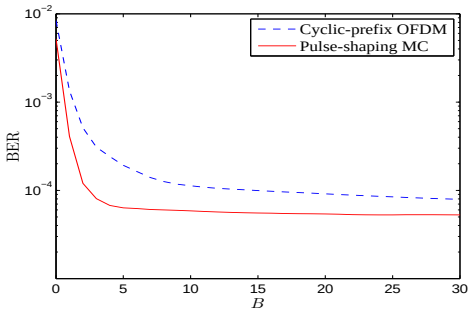

Fig. 3. *Coded BER obtained with the FD-LSQR equalizer using a pulse-shaping MC system and a cyclic-prefix OFDM system, versus the matrix bandwidth B.*

value for which the performance loss of FD-LSQR is marginal in the sense that the coded bit error rate (BER) is higher by at most 10% than for TD-LSQR (i.e., $\text{BER}_{\text{FD-LSQR}} \leq 1.1 \cdot \text{BER}_{\text{TD-LSQR}}$). The complexity ratio ρ is plotted versus $\xi_{\max}$ for different values of M, at a fixed signal-to-noise ratio (SNR) of $17\,\text{dB}$. The overall picture conveyed by Fig. 2 is that, as expected, TD-LSQR is less complex for larger maximum Doppler $\xi_{\max}$ whereas FD-LSQR is less complex for larger maximum delay M. However, when M is large (strongly dispersive channel), FD-LSQR is less complex than TD-LSQR even for larger values of $\xi_{\max}$ (high mobility).

5.2. BER performance of FD-LSQR equalization versus matrix bandwidth B; benefit of pulse shaping

Next, we compare the coded BER performance of the FD-LSQR equalizer within a pulse-shaping MC system (smooth pulses) and a cyclic-prefix OFDM system (rectangular pulses (4), (5)). The system and channel parameters are as in the previous simulation, except that we used a fixed maximum delay $M = 19$ and a fixed maximum Doppler $\xi_{\max} = 2 \cdot 10^{-3}$ (corresponding to a maximum normalized Doppler frequency of 25.6%). The transmit and receive pulses were equal ($g(n) = \gamma(n)$) and constructed as follows. A rectangular pulse of length 276 was convolved 20 times with a rectangular pulse of length 2, resulting in a smooth pulse of length 296. This pulse was orthogonalized as described in [4] (this yields a pulse with the same ISI/ICI decay characteristic, but avoids noise enhancement at the demodulation step (3) and provides perfect reconstruction).

In Fig. 3, the coded BER obtained with the FD-LSQR equalizer within the pulse-shaping MC system and the cyclic-prefix OFDM system is plotted as a function of the matrix bandwidth B, at an SNR of $17\,\text{dB}$. In both cases, $I = 15$ LSQR iterations were used. It is seen that pulse shaping can yield significant performance gains over cyclic-prefix OFDM. Specifically, the BER decay with growing B is much faster for the pulse-shaping MC system than for the cyclic-prefix OFDM system. For both systems, we see that a significant BER reduction in the FD-LSQR scheme is achieved already by the inclusion of a few off-diagonals in addition to the main diagonal.

6. CONCLUSIONS

The proposed frequency-domain LSQR equalizer using a banded approximation of the channel matrix is an iterative ICI equalization technique with low complexity and excellent BER performance. The attractive feature of the LSQR algorithm is that it achieves a regularization of the ill-conditioned channel inversion (similar in spirit to MMSE equalization) by early termination of the iteration process. The complexity of the frequency-domain LSQR equalizer can be further reduced by using pulse shaping, because smooth pulses yield a faster off-diagonal ICI decay and, hence, allow a reduction of the bandwidth used in the banded-matrix approximation. The frequency-domain LSQR equalizer is especially advantageous for rapidly varying channels with large delays.

7. REFERENCES

[1] J. A. C. Bingham, "Multicarrier modulation for data transmission: An idea whose time has come," *IEEE Comm. Mag.*, vol. 28, pp. 5–14, May 1990.

[2] S. Tomasin, A. Gorokhov, H. Yang, and J. P. Linnartz, "Iterative interference cancellation and channel estimation for mobile OFDM," *IEEE Trans. Wireless Comm.*, vol. 4, pp. 238–245, Jan. 2005.

[3] W. Kozek and A. F. Molisch, "Nonorthogonal pulseshapes for multicarrier communications in doubly dispersive channels," *IEEE J. Sel. Areas Comm.*, vol. 16, pp. 1579–1589, Oct. 1998.

[4] G. Matz, D. Schafhuber, K. Gröchenig, M. Hartmann, and F. Hlawatsch, "Analysis, optimization, and implementation of low-interference wireless multicarrier systems," to appear in *IEEE Trans. Wireless Comm.*, 2007.

[5] P. Robertson and S. Kaiser, "The effects of Doppler spreads in OFDM(A) mobile radio systems," in *Proc. IEEE VTC-1999*, (Amsterdam, The Netherlands), pp. 329–333, Sept. 1999.

[6] Y. Li and L. Cimini, "Bounds on the interchannel interference of OFDM in time-varying impairments," *IEEE Trans. Comm.*, vol. 49, pp. 401–404, March 2001.

[7] M. Russell and G. L. Stüber, "Interchannel interference analysis of OFDM in a mobile environment," in *Proc. IEEE VTC-95*, (Chicago, IL), pp. 820–824, July 1995.

[8] X. Cai and G. B. Giannakis, "Bounding performance and suppressing intercarrier interference in wireless mobile OFDM," *IEEE Trans. Comm.*, vol. 51, pp. 2047–2056, Dec. 2003.

[9] Y.-S. Choi, P. J. Voltz, and F. A. Cassara, "On channel estimation and detection for multicarrier signals in fast and selective Rayleigh fading channels," *IEEE Trans. Comm.*, vol. 49, pp. 1375–1387, Aug. 2001.

[10] L. Rugini, P. Banelli, and G. Leus, "Simple equalization of time-varying channels for OFDM," *IEEE Comm. Letters*, vol. 9, pp. 619–621, July 2005.

[11] P. Schniter, "Low-complexity equalization of OFDM in doubly-selective channels," *IEEE Trans. Signal Processing*, vol. 52, pp. 1002–1011, April 2004.

[12] W. G. Jeon, K. H. Chang, and Y. S. Cho, "An equalization technique for orthogonal frequency-division multiplexing systems in time-variant multipath channels," *IEEE Trans. Comm.*, vol. 47, pp. 27–32, Jan. 1999.

[13] T. Hrycak and G. Matz, "Low-complexity time-domain ICI equalization for OFDM communications over rapidly varying channels," in *Proc. Asilomar Conf. Signals, Systems, Computers*, (Pacific Grove, CA), Oct.-Nov. 2006.

[14] C. C. Paige and M. A. Saunders, "LSQR: An algorithm for sparse linear equations and sparse least squares," *ACM Trans. Math. Software*, vol. 8, pp. 43–71, March 1982.

[15] P. A. Bello, "Characterization of randomly time-variant linear channels," *IEEE Trans. Comm. Syst.*, vol. 11, pp. 360–393, 1963.

[16] K. Gröchenig, *Foundations of Time-Frequency Analysis*. Boston: Birkhäuser, 2001.

[17] P. C. Hansen, *Rank-Deficient and Discrete Ill-Posed Problems: Numerical Aspects of Linear Inversion*. Philadelphia, PA: SIAM, 1998.

[18] G. H. Golub and C. F. Van Loan, *Matrix Computations*. Baltimore: Johns Hopkins University Press, 3rd ed., 1996.

[19] D. Schafhuber, G. Matz, and F. Hlawatsch, "Simulation of wideband mobile radio channels using subsampled ARMA models and multistage interpolation," in *Proc. 11th IEEE Workshop on Statistical Signal Processing*, (Singapore), pp. 571–574, Aug. 2001.